Journal of Earthquake Engineering, 11:560–581, 2007

ISSN: 1363-2469 print / 1559-808X online
DOI: 10.1080/13632460601188035

Taylor & Francis
Taylor & Francis Group

Source Modeling of the Kozani and Arnea 1995 Events with Strong Motion Estimates for the City of Thessaloniki

P. SUHADOLC, L. MORATTO, and G. COSTA

Department of the Earth Sciences, University of Trieste, Trieste, Italy

P. TRIANTAFYLLIDIS

Department of Geophysics, Aristotle University of Thessaloniki, Thessaloniki, Greece

We first estimate the source parameters related to the two 1995 events near Thessaloniki (Greece): the Kozani (Ms = 6.6) and the Arnea (Ms = 5.8) earthquakes. We use the strong motion waveforms recorded in Northern Greece to retrieve by forward modeling the source characteristics of the two events. Both point-source and finite-source models are used and different 1-D velocity models tested. Due to the absence of absolute timing of most of the recordings, the modeling is limited to fitting the peak acceleration (PA) at different frequencies at the bedrock stations. The best results in terms of PA are obtained with the finite-source models for a two-asperity k-square distribution. The source model for the Kozani event is compatible with the main fault proposed by Hatzfeld et al. *[1997]. Given the two source models, we estimate the strong ground motion that would have been recorded due to these two events at different sites within the city of Thessaloniki. We estimate the strong ground motion by convolving the synthetic bedrock signals at the sites with 1-D and 2-D amplification curves obtained for the same sites during previous studies. Our analysis indicates which of the ten sites are the one most prone to strong shaking and confirms that the most crucial source parameter to be considered in ground shaking models is the rupture directivity.*

Keywords Finite-source Models; Strong Motion Estimation; Site Effects

1. Introduction

Greece is a seismically very active country due to the complex interaction between the African, Arabian, and Eurasian plates imaged by the relative movements of the Anatolian block. The Arabic plate collision against the Eurasian plate [Barka and Reilinger, 1997] involves the westward extrusion of the Anatolian block along a prominent dextral strike-slip fault that continues in the North Aegean (North Aegean trough). These plate motions cause the seismicity to be among the highest in Europe, particularly in the area of the South Aegean Sea and along the Hellenic trench. In the latter two regions, the mechanisms are mainly compressional, whereas in the area of North Aegean Sea and North Anatolia the principal mechanism is the dextral strike-slip. In Northern Greece the seismicity is lower and the focal mechanisms are principally extensional because of the counter-clockwise rotation of Anatolia with respect to Eurasia.

Received 5 June 2006; accepted 22 December 2006.
Address correspondence to P. Suhadolc, Department of the Earth Sciences, University of Trieste, Via E. Weiss 1, 34127 Trieste, Italy. E-mail: suhadolc@units.it

In Northern Greece, two important earthquakes, Arnea and Kozani, occurred in 1995. The Kozani earthquake is well investigated [e.g. Hatzfeld *et al*., 1995, 1997; Pavlides *et al*., 1995; Meyer *et al*., 1996; Clarke *et al*., 1997], whereas there are only a few studies of the Arnea event [Margaris and Hatdizimitriou, 1997; Hatzidimitriou, 2003].

The Arnea event occurred on May 4, 1995. The hypocenter was estimated by Harvard at 40°32′ 27″ N, 23°38′ 2.4″ E with a depth of about 15 km, magnitude values Mw = 5.3, Ms = 5.8, Mb = 6.0 and focal mechanism $\theta = 260°$, $\delta = 42°$, $\lambda = -132°$. Hatzidimitriou [2003] proposed a different focal mechanism for dip and rake, $\theta = 260°$, $\delta = 80°$, $\lambda = -170°$, and he estimated different values for the hypocenter depth (9 km). Margaris and Hatdizimitriou [1997] estimated the fault length to be 12.5 km.

The Kozani earthquake on May 13, 1995 was the strongest event occurred in Northern Greece since about ten years. It was preceded by five foreshocks and the main shock occurred at 8:47 GMT. Harvard hypocenter position is at 40°9′36″ N, 21°40′12″ E, depth = 9 km, and the focal mechanism $\theta = 243°$, $\delta = 47°$, $\lambda = -97°$. Pavlides *et al*. [1995] made a geological study and Meyer *et al*. [1996] were able to use SAR interferometric data because of the size of the event. Clarke *et al*. [1997] inverted geodetic data and found the coseismic movement and the source parameters: focal mechanism, $\theta = 253°$, $\delta = 43°$, $\lambda = -95°$, the depth of the fault (between 3 and 13 km) and a seismic moment larger than seismic moment proposed with seismological studies. Hatzfeld *et al*. [1995, 1997] studied the aftershocks distribution; they estimated the magnitude value, Ms = 6.6, and the focal mechanism, $\theta = 252°$, $\delta = 41°$, $\lambda = -87°$. They also proposed unilateral rupture propagation from NE to SW, placing the nucleation at the NE corner of the fault, near Kozani. The inversion gave a source function with two impulses, the first one being bigger than the second one with a few seconds separation between the two. Moreover, the aftershocks locations evidenced a cluster delineating a plane that dips southward, opposite to the main cluster. Hatzfeld *et al*. [1995, 1997] therefore proposed the presence of an antithetic fault smaller than the main fault, its extension being about the 8% of the main fault surface and producing the 15% of the total seismic moment.

The aim of this study is to determine which of the above earthquake parameters provides the best fit for the amplitudes of accelerograms recorded near the source of these two events and to estimate, taking into account the local site conditions, the shaking motion at different localities within the city of Thessaloniki (Greece) due to the two events.

2. Methodology

The first step of this study is modeling the seismic source parameters of the Kozani and Arnea 1995 events; generally, to model the fault and to estimate the distribution of the slip on the surface an inverse procedure is adopted. These slip models are derived from relatively long period data (strong motion velocity and displacement, and teleseismic velocity seismograms) because, at these long periods, ground motions are predominantly deterministic and their waveforms can be accurately modeled. Because in the area no other recordings are available, we use in this study only accelerometric data recorded, however, without the absolute time and therefore, we cannot solve the inverse problem. We therefore model the peak acceleration applying a trial and error method (forward problem) based on the selection of different values for the most important source parameters and choosing the result having the smallest misfit.

The second step of this study is estimating strong motion at different localities within the city of Thessaloniki due to the Kozani and Arnea 1995 events taking into account the site effects. Strong motion estimates require knowledge about the seismic source, structural

model, and site response and they can be evaluated applying a probabilistic (using ground-motion relations) or deterministic approach (computing synthetic seismograms).

Ground-motion relations allow us to estimate the earthquake ground motion as a function of magnitude, distance from the source, and geology of the receiver site; the ground shaking motion can be represented by several parameters (peak ground acceleration, peak ground velocity, spectral acceleration, Arias intensity) [e.g. Douglas, 2003]. Nowadays there are a large number of different models and different parameters for estimating ground motion on a global scale, limited to a regional or local area, for a particular type or class of earthquake mechanisms [Campbell, 1981, 1997]. Different laws are, for example, proposed for California [e.g. Joiner and Boore, 1981; Newmark and Hall, 1982; Boore *et al*., 1997; Boatwright *et al*., 2003], for the Washington-Alaska area [Youngs *et al*., 1997], for Europe [Ambraseys and Simpson, 1996; Ambraseys *et al*., 1996] and the Middle East area [Ambraseys *et al*., 2005]. Fault mechanisms characterization has recently been included in ground motion estimation relations [Abrahamson and Silva, 1997; Campbell 1997; Spudich *et al*., 1999; Ambraseys and Douglas, 2003; Ambraseys *et al*., 2005; Zhao *et al*., 2006a]. At the same time regression analysis has been further developed refining the theoretical models and the computation algorithms [e.g. Joyner and Boore, 1993] and including site effects [Kanno *et al*., 2006; Zhao *et al*., 2006a, b]. We compared our synthetic signals with estimations made using European relations [Ambraseys and Simpson, 1996; Ambraseys *et al*., 1996].

Numerous methods of synthesizing seismograms numerically from source and wave theory in the vicinity of a large seismic source have been published [e.g. Irikura, 1983; Bolt, 1987; Bolt and Abrahamson, 2003]. Because the computation of site-dependent and phased-time histories is not unique, a number of alternative methods are available [e.g. Gusev, 1983; Vidale and Helmberger, 1987; Mikumo and Miyatake, 1987; Panza and Suhadolc, 1987; Joyner and Boore, 1988]. In areas where the geology of the soil is known in detail, 3-D structural models have been selected; this is the case of California region and of Japan [e.g. Pitarka, 1999; Irikura *et al*., 2004]. In this study, synthetic seismograms are computed in Thessaloniki city applying the modal summation technique [Panza, 1985; Panza and Suhadolc, 1987; Florsh *et al*., 1991]. Arnea and Kozani sources are modeled using parameters obtained in the first part of the study. A mono dimensional structural model is selected because of the scarse knowledge of the region geology and to limit the computation time. At last we convolve the synthetic signals computed on bedrock with specific site characteristic amplification curves [Triantafyllidis *et al*., 2001, 2002, 2004a, b], considering in this way the local site effects. Applying this procedure, peak ground accelerations are computed in a frequency range of engineering interest by taking into account the complexity of extended seismic sources and the local conditions at the receivers.

3. Data Process

In this study we model the Arnea and Kozani seismic sources to fit the acceleration amplitudes at nearby strong motion stations since these are the only data available in the near source region and are most sensitive to source rupture properties. Based on these source models we compute the signals related to the two events in the city of Thessaloniki, taking into account in a simplified way also site effects. We have downloaded the strong motion data from the ISESD [Ambraseys *et al*., 2002] website (http://www.isesd.cv.ic.ac.uk/ESD). As already mentioned the lack of the absolute time in the recording forced us to use a trial and error technique in the modeling.

We are interested in estimating the principal source parameters of the 1995 Arnea and Kozani earthquakes: focal mechanism, depth of hypocenter, magnitude, fault dimension,

rupture propagation, and seismic moment distribution. We calculate synthetic seismograms with the modal summation technique [Panza 1985; Panza and Suhadolc, 1987; Florsh *et al*., 1991] applying at first a point-source model and subsequently a finite-source model [e.g., Das *et al*., 1996]. The related structural models are representative of the region around the source [Papazachos *et al*., 1966; Christodoulou and Hatzfeld, 1988; Papazachos *et al*., 1995; Tselentis *et al*., 1996; Papazachos and Nolet, 1997; Papazachos, 1998; Tselentis, 1998; Zahradnik and Papatsimpa, 2001; Novotny *et al*., 2001; Karagianni *et al*., 2002].

When comparing observations and computations we choose the model with the lowest misfit values. The misfit values are calculated for each record as the ratio between the peak acceleration (PA, maximum frequency content at 1 Hz for Kozani event and 3 Hz for Arnea event) on the horizontal components of the observed data (o_i) with respect to the PA on horizontal components of the synthetic records (s_i), and the total misfit for the entire number of records (N) given by:

$$\chi = \frac{1}{N}\sum_{i=1}^{N}\frac{(o_i - s_i)^2}{o_i^2} \tag{1}$$

First, we estimate the value of magnitude, the depth of the hypocenter, the focal mechanism, and the best structural model (only for the Arnea event) using the point-source model, since these parameters represent centroid properties. Epicentral locations are kept fixed because this parameter is relatively stable, whereas focal mechanisms and magnitude values are extracted from previous studies.

Later on we fix all parameters obtained with the point-source model assuming them constant over the entire rupture area and we estimate the fault details (fault dimensions, the nucleation position, and the type of seismic moment distribution) with extended source models. The estimates of the fault dimensions are made using both aftershocks distributions (time interval of 2 days, 1 week, and 1 month after the main shock) and the empirical relations proposed by Wells and Coppersmith [1994]. The nucleation positions are fixed in the zone of interest of the surface area (in the middle, at the farthest limits, etc.) and different seismic moment distributions on the fault are used: a uniform smoothed-at-the-borders distribution, a distribution with one asperity, and two distributions with two asperities, all asperities being modeled with a k^2 distribution [Herrero and Bernard, 1994].

We also tried to numerically compare the synthetic and observed waveforms, but this was found to be hardly possible because the records do not have the absolute time or a pre-trigger time. We have tried to calculate the theoretical arrival time of P- and S-waves using a ray-tracing program [Jansky, 1994] but the results did not help much to estimate an absolute time on the records. Therefore, in order to choose the best model, we take into account the total misfit, the PA ratios and a visual comparison of the observed and synthetic waveforms.

Ground-motion relations [Ambraseys *et al*., 1996; Ambraseys and Simpson, 1996] have been also used to estimate the peak spectral horizontal acceleration (SA_H) and the peak spectral vertical acceleration (SA_V) and we compare these estimates with our results. The relation is (the coefficients C_i are reported in Table 1 of Ambraseys *et al*., 1996, and Ambraseys and Simpson, 1996):

$$\log(SA_{H,V}) = C_1 + C_2 M + C_4 \log(r) + C_A S_A + C_S S_S \tag{2}$$

TABLE 1 Coordinates of the ten receivers in the city of Thessaloniki where amplification curves had been computed by Triantafyllidis *et al*. [2001, 2002]

Station	Latitude (N)	Longitude (E)
AMP	40° 39′ 36″	22° 54′ 50″
OTE	40° 38′ 29″	22° 56′ 06″
ROT	40° 38′ 06″	22° 57′ 11″
LEP	40° 37′ 37′	22° 56′ 56″
LAB	40° 37′ 44″	22° 57′ 40″
POL	40° 35′ 49″	22° 57′ 22″
TYF	40° 36′ 50″	22° 57′ 11″
OBS	40° 37′ 55″	22° 57′ 54″
KAL	40° 34′ 52″	22° 56′ 53″
AGO	40° 38′ 20″	22° 56′ 36″

where M is the surface magnitude and r the hypocentral distance. The last two terms are selected according to the soil type on which the station is placed: stiff soil ($S_A = 1$) or soft soil ($S_S = 1$). The results obtained with ground-motion relations are compared with PA extracted from recordings and synthetic seismograms.

Finally, we compute the signals in ten selected receivers in the city of Thessaloniki using the best models found with the point-source and the finite-source approximation for the Arnea and Kozani earthquakes. To estimate the strong ground motion that would have been recorded by these two events at different sites in the city we convolve the synthetic signals computed on bedrock with 1-D and 2-D site-specific amplification curves obtained by Triantafyllidis *et al*. [2001, 2002, 2004a, b]. These amplification curves have been computed for ten selected sites in Thessaloniki city (Table 1, Fig. 1) applying both 1-D (upper frequency of 10 Hz) and 2-D models (upper frequency of 6 Hz). The mean ratio between the amplitude FT of the synthetic seismograms computed at different azimuth and distance from the seismic source using both regional and local structural models provides the amplification curves at each receiver. The regional structural model is one-dimensional while local structural models vary vertically for the 1-D case and also horizontally for the 2-D case. We compute our synthetic seismograms as accelerations with the modal summation technique [Panza, 1985; Panza and Suhadolc, 1987; Florsh *et al*., 1991] and, after the convolution, the peak ground acceleration is extracted. Accelerograms are used, since the synthetic signals computed by Triantafyllidis *et al*. [2001, 2004a, b] and used to estimate the site amplification were accelerograms too. For each earthquake the highest P1HA (peak acceleration with maximum frequency content of 1 Hz) is extracted at all selected sites giving us an estimation of the relative hazard (the level produced by the 1995 Arnea and Kozani events) for the city of Thessaloniki.

4. The 1995 Arnea Earthquake

Strong motion records [Ambraseys *et al*., 2002] from four stations are used to model the Arnea event: Poligiros, Ierissos, Profitis, and Agios Basilios. Poligiros and Profitis are bedrock stations; Ierissos is placed on stiff soil, whereas the type of soil at Agios Basilios is unknown. All stations are located at a distance between 20 and 45 km from the epicenter and there is no observed data NE from the event.

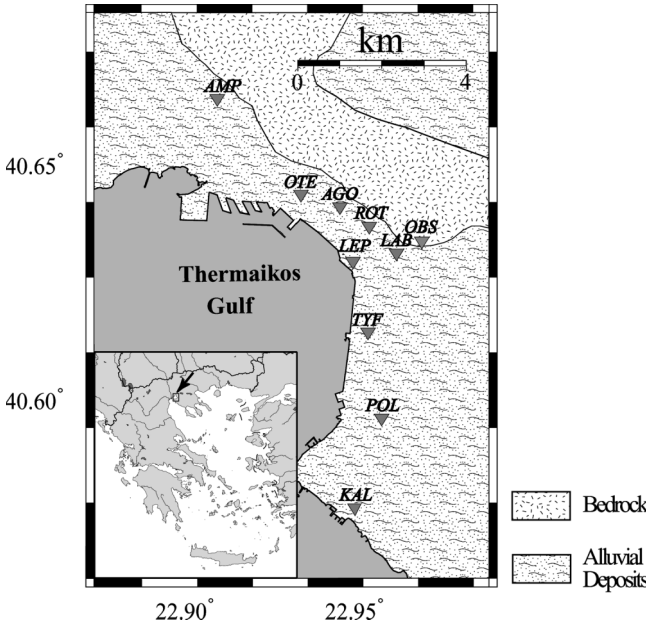

FIGURE 1 The receivers in the city of Thessaloniki where the 1-D and 2-D amplification curves were computed.

We use two different velocity models called “mygdonia” and “volvi” to compute synthetics. A velocity model is derived from Papazachos (personal communication) who has provided velocity values taken from Papazachos and Nolet [1997] until 137 km depth, but with no velocity values in the first kilometer. Estimates for the velocities in the first kilometer are taken from the Marrara and Suhadolc [1998] valid for the Volvi area. We have decided to use two structural models differing only in the first kilometer value: the P-wave velocity value 4 km/s from Marrara and Suhadolc [1998] led to the “volvi” model, the 4.85 km/s value obtained extending to the surface the velocity value at 1 km of depth led to the “mygdonia” model. The Poisson ratio was used to infer S-wave velocities.

For the Arnea earthquake we calculate the synthetic seismograms for an upper frequency cutoff of 10 Hz. We have decided, however, to filter the signals with an upper frequency cutoff of 3 Hz because the signal/noise ratio is not good for higher frequencies and because the available structural models are not known with sufficient detail to allow for meaningful results at higher frequencies.

The number of recorded aftershocks is small and so their positions did not give us a good estimate of fault dimension. All aftershocks locations are placed S to SW of the mainshock epicenter suggesting that the rupture front propagated from NE to SW and that the nucleation was at the NE end of the fault.

We kept the epicenter position (40°35′59″ N, 23°36′00″ E) fixed when using the point-source approximation, because all previous studies are in agreement with these values. We determine the source model by analyzing 36 different models: we consider three values for depth (6 km, 9 km, and 12 km), three values for magnitude (5.4, 5.6, and 5.8), two different focal mechanisms (proposed by Harvard and by Hatzidimitriou [2003] respectively) and two different velocity models (“mygdonia” and “volvi”). The synthetic seismograms are computed for all these 36 models and then we estimate the total misfits and the P3HA (peak acceleration with maximum frequency content of 3 Hz) ratios. The

comparison indicates that the best model has the focal mechanism proposed by Harvard (θ = 260°, δ = 42°, λ = –132°), the structural model called "mygdonia" (V_p = 4.85 km/s) and the magnitude value 5.8. We have also decided to determine the best hypocenter depth proposing 8 models where only the source depth varied (from 5–12 km). In the best model (total misfit = 0.295), the hypocentral depth is 7 km.

With the basic point-source parameters determined, we calculate synthetic seismograms with finite-source models. We use all results obtained with the point-source models and place the nucleation point on the epicenter position, with the center of the fault put at 7 km depth. Three pairs of values for fault dimensions (length L = 10 km, width W = 5 km; L = 12 km, W = 6 km; L = 13 km, W = 7 km) are considered based on source scaling laws [Kanamori and Anderson, 1975; Wells and Coppersmith, 1994]. The nucleation is placed at five different locations (from E towards W) in the deeper part of the fault: 0.00 × L; 0.25 × L; 0.50 × L; 0.75 × L; 1.00 × L. At the beginning we have chosen four different seismic moment distributions: a uniform smoothed-at-the-borders distribution, a distribution with one asperity, and two distributions with two asperities, all asperities being modeled with a k^2 distribution [Herrero and Bernard, 1994]. The best misfit with a value 0.192 is obtained for the model with fault dimensions 10 km × 5 km, the nucleation placed at 0.25 × L, and with a uniform seismic moment distribution smoothed at the borders. All models with fault dimensions 13 km × 5 km yielded the best results in relation to the P3HA ratio and waveform resemblance. We therefore fix the fault dimensions (L = 13 km, W = 7 km) and investigate ten different seismic moment distributions: four seismic moment distributions are flat and smoothed at the border with different values of smoothing, three seismic moment distributions have one or two asperities modeled with the k^2 law [Herrero and Bernard, 1994], and three seismic moment distributions have one or two asperities modeled with a simple cosine law. The model with nucleation placed at ¼ of the fault from E towards W (0.25 × L) and with one asperity modeled with the k^2 distribution provide the best results for both the P3HA ratios and waveform resemblance.

The modeling results for the 1995 Arnea earthquake yielded two best source models: the first model has a smaller fault area (L = 10 km, W = 5 km) and a uniform seismic moment distribution smoothed at the borders (with a smoothing value of 20 % of the fault area), whereas the second model (Fig. 2) has a larger area (L = 13 km, W = 7 km) and a seismic moment distribution with one asperity, modeled with the k^2 law, placed in the middle of the fault. In both models the nucleation is placed at ¼ of the fault length from E towards W. The first model provides the best misfit values, whereas the second one gives the best P3HA ratios and waveforms. In source modeling the fault area and the seismic moment distribution are related: models with flat seismic moment distribution on a smaller fault area and models characterized by one asperity on a larger fault area produce similar values of P3HA. Both models are acceptable for the 1995 Arnea source and both models are in agreement with the observed data considered.

Finally, we compare the P3HA values obtained from recordings with the SA values at 3 Hz derived using ground-motion relation (2), denoted as "empirical data," and with the synthetic data using point-source and finite-source models. These values for all stations (horizontal and vertical components) are plotted in Fig. 3. At Profitis station observed and synthetic data are in agreement, whereas site effects appear to be important at stations Ierissos and Agios Basilios, where the P3HA values extrapolated from synthetic data are smaller than those obtained from observations. It is interesting to note the directivity effect at the Poligiros station: the finite-source values (particularly the model with fault area 13 km × 7 km) are in agreement with observations, whereas the values derived from point-source models are too small. In fact, Poligiros station is placed in the direction of rupture propagation, so the directivity is important and only a finite-source model can reproduce synthetic seismograms having this effect.

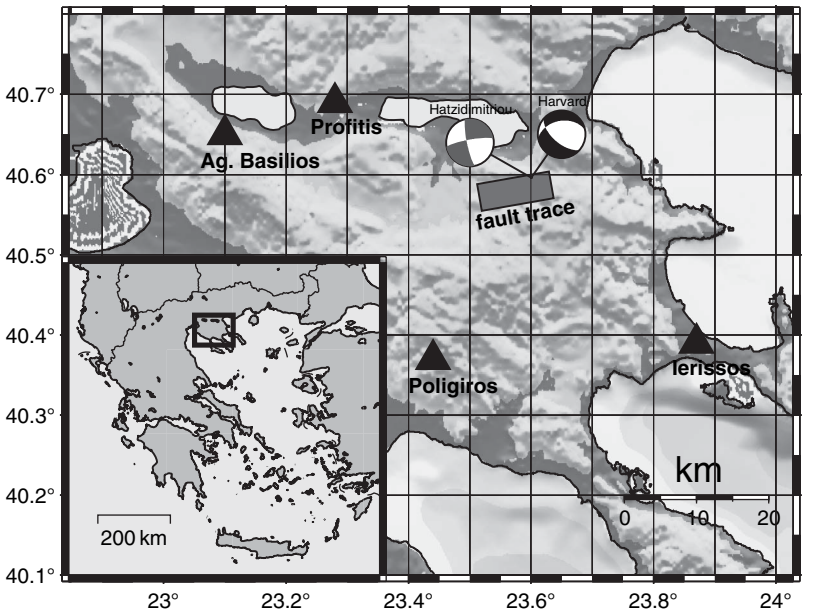

FIGURE 2 The map of Arnea earthquake area; the triangles are strong motion stations and the dark rectangle is modeled fault plane.

The final results are summarized in Table 2. The epicenter position is fixed and the hypocenter depth (7 km) is derived from the point-source modeling. In the finite-source modeling we fix this latter value in the center of the fault area where the largest seismic moment is released. The best focal mechanism according to our analysis is that proposed by Harvard, an extensional mechanism with a small part of left-lateral slip. The rupture propagated principally from W towards E, in agreement with aftershocks locations and the directivity pulse seen at Poligiros, and "mygdonia" is the velocity model giving the best results. Two different models with similar P3HA values have been obtained from finite-source modeling: in the first model the fault area is 10 km large and 5 km wide and the seismic moment distribution is uniform and smoothed at the borders. In the second model the fault area is 13 km large and 7 km wide (in agreement with Margaris and Hatdizimitriou, 1997), the seismic moment distribution having one asperity modeled with the k^2 law. Both models are supported by the data we have considered.

5. The 1995 Kozani Earthquake

Strong motion data [Ambraseys *et al*., 2002] from eight stations that have recorded the 1995 Kozani event are taken into account: Edessa, Florina, Karditsa, Kastoria, Katerini, Kozani, Larissa, and Veria. Florina, Kastoria, Kozani, and Veria are stations placed on rock, whereas the other four stations are placed on stiff soil. Seven stations are placed at distances between 50 and 93 km from the earthquake epicenter, while Kozani station is placed only 17 km from the epicenter. Unfortunately, there is no station placed SW of the event, in the direction all previous studies propose the earthquake rupture propagates.

We adopt only one velocity model (denoted "kozani") to investigate the Kozani event. Papazachos (personal communication) provided us with the velocity values until

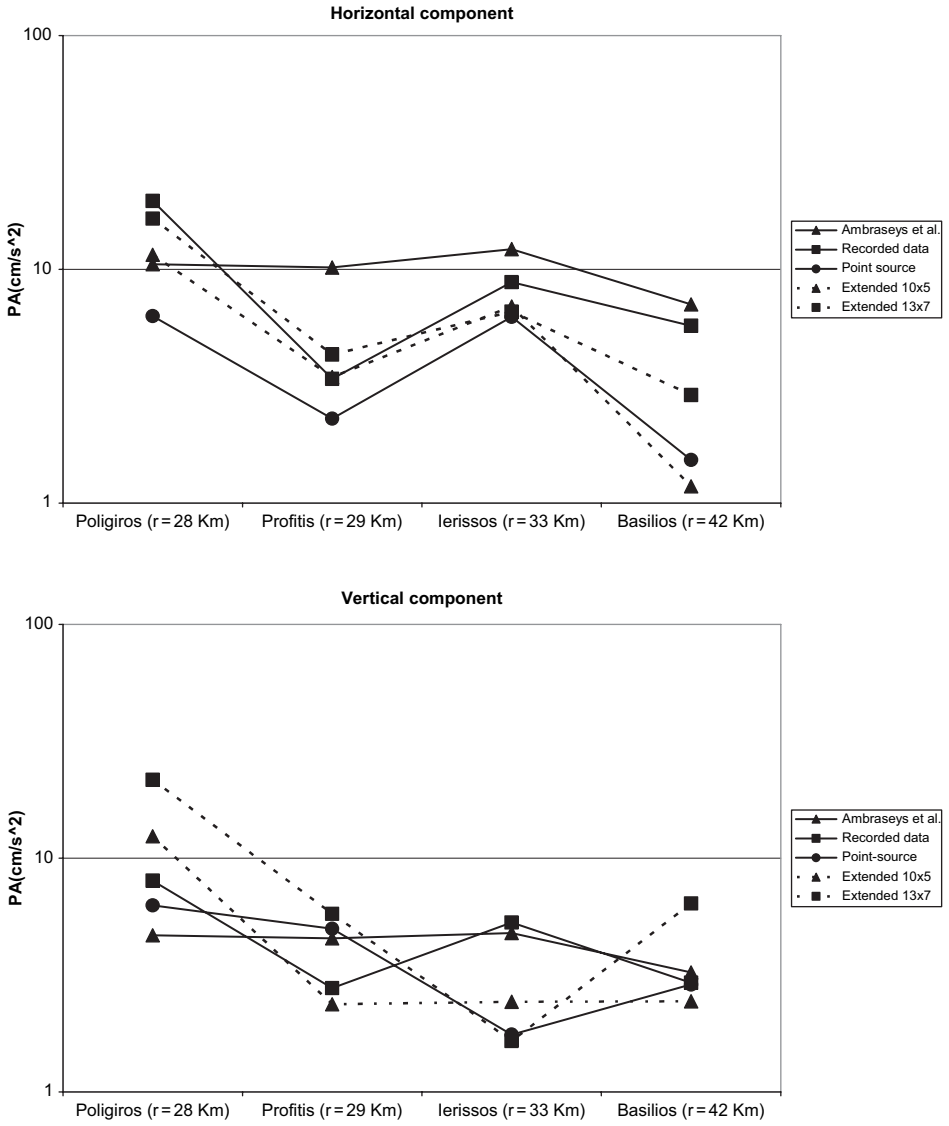

FIGURE 3 The comparison of Peak Acceleration values (PA) for the horizontal (top) and the vertical (bottom) component due to the Arnea earthquake retrieved from recordings (P3HA), synthetic seismograms (P3HA) and ground-motion relations (SA at 3 Hz) [Ambraseys *et al*., 1996; Ambraseys and Simpson, 1996].

137 km depth [Papazachos and Nolet, 1997], but no values for the first two kilometers. We use a P-wave velocity value 4.50 km/s at the surface proposed by Drakatos *et al*. [1998].

The synthetics are computed with an upper frequency cutoff of 1 Hz. The data are low-pass filtered with an upper frequency cutoff of 1 Hz, the signal/noise ratio being good at all stations. The number of recorded aftershocks is big, their locations being mostly placed SW and S of the epicenter suggesting that the rupture front propagated from NE to SW and that the rupturing was unilateral, all in agreement with the results of previous

TABLE 2 Final results obtained from source modeling of Arnea event using point source and finite source

Epicenter latitude	40° 35′ 59″ N
Epicenter longitude	23° 36′ 00″ E
Centroid depth	7 km
Strike	260°
Dip	42°
Rake	228°
Magnitude	5.8
Nucleation position	0.25 × L
Fault area	(10 × 5 km) – (13 × 7 km)
Seismic moment distribution	(flat and smoothed) – (1 asperity)
Structural model	"mygdonia"

studies. The aftershock distribution also suggests that there might be an asperity placed near the nucleation at the NE part of the fault.

Again we keep the epicenter position (40°10′59″ N, 21°39′36″ E) fixed when using the point-source approximation because all previous studies agree with these values. We choose three values for the hypocentral depth (9 km, 12 km, and 15 km), two values for the magnitude (6.5 and 6.6), and three different focal mechanisms [proposed by Harvard, Clarke *et al*., 1995; Hatzfeld *et al*., 1997] leading to 18 models. The total misfit indicates that the magnitude value is 6.6 and excludes models with the 12 km source depth. This is in agreement with previous studies that proposed the nucleation to be 15 km deep with an asperity releasing much seismic moment at a depth of 9 km. The P1HA ratios indicate that the best point-source depth is 9 km. We use only the P1HA ratios at bedrock stations in the analysis, because the synthetic seismograms at the other stations (placed on "stiff soil" and with evident site effects) yield us too small values. Models with the three different focal mechanisms yield similar results, so we use the comparison of synthetic and observed waveforms to choose the "best" model: the focal mechanism, $\theta = 253°$, $\delta = 43°$, $\lambda = -95°$, proposed by Clarke *et al*. [1997].

Next we compute synthetic seismograms with finite-source models using all the results obtained with the point-source analysis and placing the nucleation at the epicenter position. Since much seismic moment appeared to be released 9 km deep, we place the nucleation somewhat deeper, at 12 km. Three pairs of values for fault dimensions are considered (L = 18 km, W = 9 km; L = 20 km, W = 10 km; L = 25 km, W = 17 km) according to scaling laws [Kanamori and Anderson, 1975; Wells and Coppersmith, 1994] and the related stress drop values vary between 24 and 105 bars. The nucleation point is fixed at the NE corner of the fault in its deepest part in agreement with all previous studies. Again, three different seismic moment distributions are considered: a uniform distribution smoothed at the borders, a distribution with one asperity modeled with the k^2 law [Herrero and Bernard, 1994], and a distribution with one asperity modeled with a simple cosine law. The total misfit value excludes the last seismic moment distribution, and the P1HA ratios and waveform comparison indicates that the best model fault dimensions are 18 km × 9 km (Fig. 4). We therefore fix these values and study the seismic moment distributions in more detail considering seven distributions: a uniform one smoothed at the border, three distributions with one or two asperities modeled with the k^2 law [Herrero and Bernard, 1994] and three distributions with one or two asperities modeled with the cosine law. The "best" model found has a seismic moment distribution with two asperities modeled with the k^2 law with the larger asperity placed near the nucleation (Fig. 5).

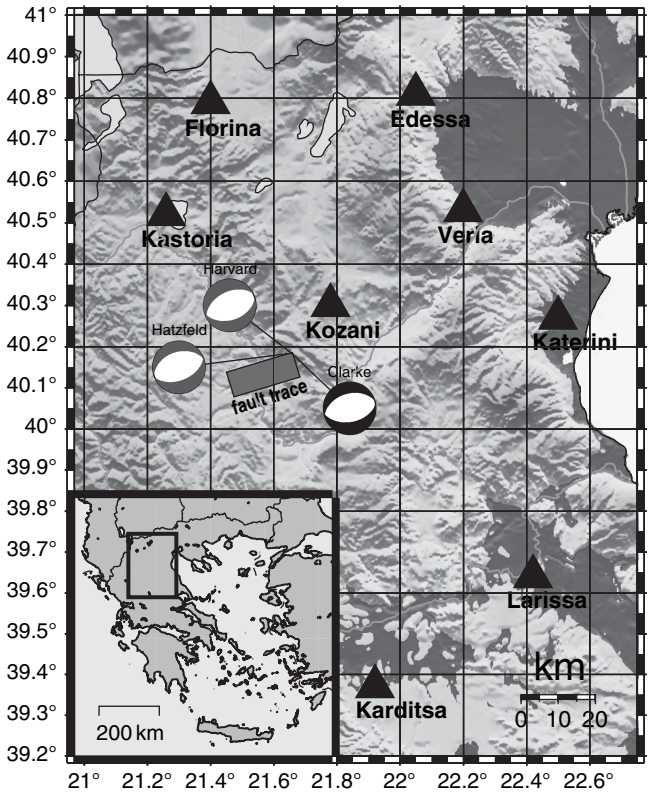

FIGURE 4 The map of Kozani earthquake area; the triangles are strong motion stations and the dark rectangle is modeled fault plane.

Hatzfeld *et al*. [1997] suggest the presence of an antithetic fault for the Kozani event: they propose a secondary event with a fault area 8% of the main fault and with a seismic moment 15% of the total seismic moment related. The antithetic fault began to slip 6.5 s after the main fault nucleation time and this secondary event is placed to the NW between the city of Kozani and Grevena. In agreement with this analysis we place the hypocenter of secondary event to the NW of main shock (40°18′00″ N, 21°32′36″ E, depth = 10.5 km) and we choose for it an extensional focal mechanism (θ = 90°, δ = 40°, λ = 270°). Although the information about the secondary event is poor, both the considered fault area (L = 8 km, W = 5 km) and the magnitude value (derived taking 15% of the total seismic moment) used in our modeling are in agreement with previous studies.

The summing up of the main shock signals with the secondary event ones resulted in too high P1HA values, since the total moment was too big when adding the antithetic fault subevent to the unmodified point-source derived seismic moment. Therefore, we increase the dimensions of the main fault to L = 25 km and W = 17 km, in order to decrease the stress drop and get the correct P1HA values.

The antithetic fault is modeled with a finite source and eight different models are constructed with different seismic moment distributions and nucleation locations. The nucleation is placed in the center of the fault or at its eastern end (near Kozani), and the considered distributions are either uniform and smoothed at the borders or containing one or two asperities modeled with the k^2 law. The total misfit values and the P1HA ratios

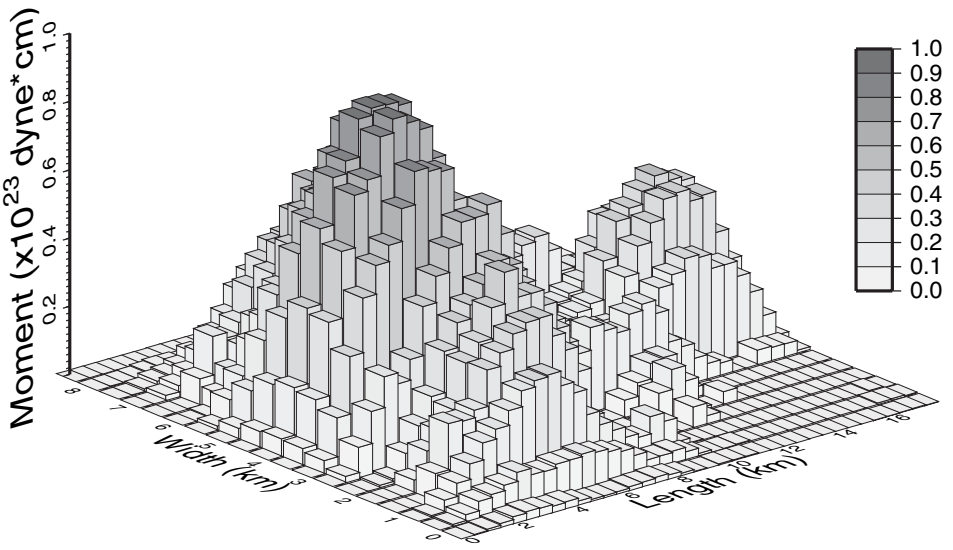

FIGURE 5 The seismic moment distribution for the Kozani event; there are two asperities modeled with k^2 law [Herrero and Bernard, 1994] and the greater asperity is placed at NE, near the city of Kozani.

indicate that in the best model the nucleation is placed at the eastern end of the fault (Fig. 6) and that the seismic moment distribution has two asperities modeled with the k^2 law.

Finally, we compare the P1HA values obtained from recordings and synthetic data using point-source and finite-source models, with SA values at 1 Hz derived from empirical data (using ground motion relation (2)). These values (horizontal and vertical components) are plotted in Fig. 7 for all stations. There is a good agreement at Edessa and Florina, whereas the amplification due to site effects at Katerini and Larissa is quite evident. At Kastoria the antithetic fault rupture produces stronger than observed P1HA, but

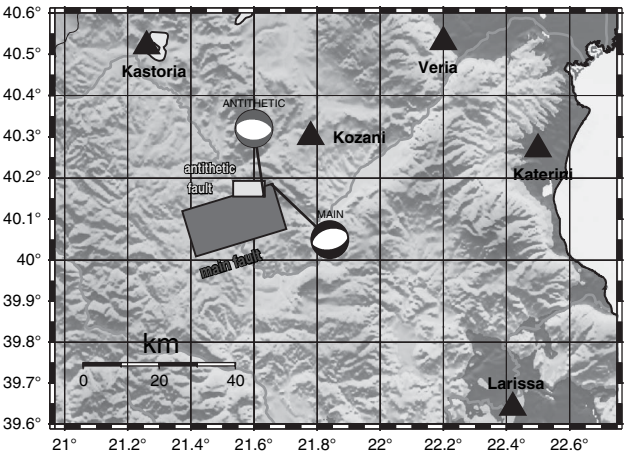

FIGURE 6 The map of Kozani main fault (dark rectangle) and antithetic fault (light rectangle); the triangles are strong motion stations.

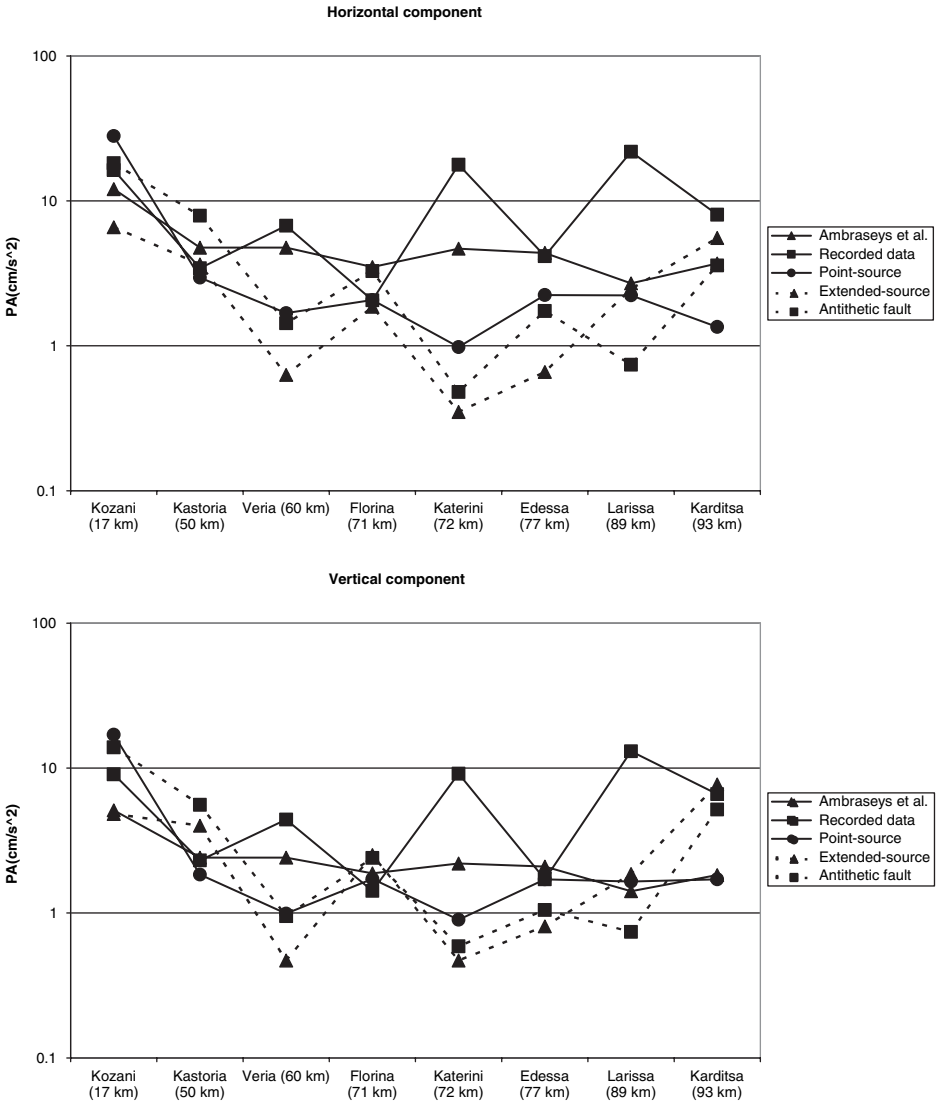

FIGURE 7 The comparison of Peak Acceleration values (PA) for the horizontal (top) and the vertical (bottom) component due to the Kozani earthquake retrieved from recordings (P1HA), synthetic seismograms (P1HA) and ground-motion relations (SA at 1 Hz) [Ambraseys *et al*., 1996; Ambraseys and Simpson, 1996].

the P1HA at other stations are in agreement with recordings. Veria is considered a bedrock station but it might have some site effects due to the "generic" rock heterogeneities [Douglas *et al*., 2004]. Kozani is a bedrock station placed near (17 km) the source so the directivity effect can be important. At Kozani the antithetic fault yields a P1HA in agreement with the recorded one, whereas the point-source P1HA are too high and the finite-source P1HA with no antithetic fault subevent are too small.

The final results are given in Table 3. The epicenter position is fixed and the hypocenter depth (9 km) is derived from the point-source modeling. In the finite-source modeling we fix this latter value in the center of the fault area where the largest seismic moment is released. The best focal mechanism according to our analysis is the extensional mechanism

TABLE 3 Final results obtained from source modeling of Kozani event using point source and finite source

Epicenter latitude	40° 10′ 59″ N
Epicenter longitude	21° 39′ 36″ E
Hypocenter depth	12 km
Strike	253°
Dip	43°
Rake	265°
Magnitude	6.6
Nucleation position	NE
Fault area	(18 × 9 km)
Seismic moment distribution	(2 asperities)
Structural model	"kozani"

proposed by Clarke *et al*. [1997]. The nucleation position at the NE end of the fault is also kept fixed being in agreement with all previous studies and the aftershocks locations. The selected velocity model is "kozani" and the assigned magnitude 6.6. The one-fault finite-source analysis suggests a fault area 18 km × 9 km with a k^2-law seismic moment distribution characterized by two asperities, the larger one being placed in the northeast part of the fault. In the two-fault finite-source analysis (which includes the antithetic fault) the main fault area is 25 km × 17 km and the antithetic fault area 8 km × 5 km. The nucleation of the extensional subevent is placed NW from the main shock. Again a k^2-law seismic moment distribution characterized by two asperities gives the best results.

The antithetic fault rupture contributes also some relatively high frequencies to the signal in agreement with the observed waveforms, so we consider the two-fault finite-source model as the best one.

Figure 8 shows, as an example, the comparison between signals recorded at the Kozani station and synthetic seismograms computed at the same receiver applying the extended source model and assuming the presence of the antithetic fault: we consider the agreement observed on the two horizontal components, where the amplitudes are comparable and the waveforms are roughly similar, as acceptable.

6. Strong Motion Estimates in Thessaloniki

The source models for the 1995 Arnea and Kozani events are used to compute synthetic seismograms at ten selected sites within the city of Thessaloniki. The signals are first calculated for bedrock ground conditions and subsequently convolved with 1-D and 2-D mean amplification curves obtained by Triantafyllidis *et al*. [2001, 2002, 2004a,b] to account for site effects. The receivers distance is around 120 (± 3) km for the Kozani earthquake and 56 (± 3) for the Arnea event.

The velocity model "mygdonia" is used to compute the signals generated by the Arnea source model. Two signals are computed, based on the point-source and finite-source models.

In the Kozani case the point-source model and the finite-source models with and without the presence of antithetic fault are considered. For the velocity model both the "kozani" model and a new regional velocity model "grepap" are used. The "grepap" model is also based on the Papazachos and Nolet [1997] data in the upper 137 km and the missing values in the first kilometer of depth are replaced with those at 1 km depth resulting in a regional velocity model quite fast near the surface.

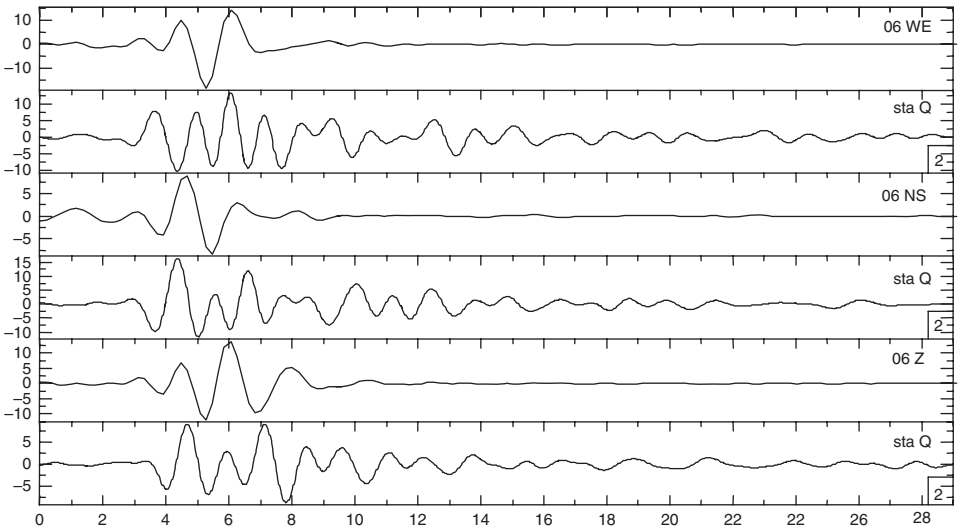

FIGURE 8 The comparison between the synthetic seismograms computed adopting the extended source model with the antithetic fault and the signals recorded at the Kozani station. The order of the signals from top is: East synthetic, East recording, North synthetic, North recording, vertical synthetic, and vertical recording.

The P1HA values on bedrock obtained within Thessaloniki for the best Arnea and Kozani source models have about the same value at all stations because they are calculated for bedrock ground conditions (no site effects) with small differences due to slightly different azimuths and distances from the sources. After the signals are convolved with the mean amplification curves estimating the site effects at the selected localities obtained by Triantafyllidis *et al*. [2001, 2002, 2004a,b] the P1HA values differ considerably from station to station. Triantafyllidis *et al*. [2001, 2002, 2004a,b] obtained the amplification curves using both 1-D and 2-D velocity models and the Fourier spectra ratios. In the 1-D case the ratios between the Fourier spectra of signals have been computed using 1-D local soil profiles, while in the 2-D case a vertically and horizontally heterogeneous local soil has been selected; the regional structural model is only vertically heterogeneous. The amplification curves were computed for an upper frequency cutoff of 10 Hz for the 1-D models and for an upper frequency cutoff of 6 Hz for the 2-D models.

We compare the signals due to the Arnea and Kozani source models for an upper frequency cutoff of 1 Hz. Only horizontal components are compared because these are the components most influenced by site effects. We choose the strongest P1HA values between all models for every seismic event component (North and East) and plot them in Fig. 9 for all stations. Figure 9 shows how differently the various sites are affected by the two events (different distances, azimuth and source parameters); examples are stations TYF and KAL which show very different amplification levels for the two events. Both events produce higher accelerations at POL, TYF, and KAL indicating these sites as the most dangerous (among the areas considered) in the city of Thessaloniki in terms of seismic hazard. Generally, the North component has higher P1HA values than the East one for all stations in Thessaloniki; it is interesting to notice the difference in P1HA values between the two horizontal components of the Arnea event at stations POL and KAL. The source therefore strongly influences the amplification at a site (as it is shown from the differences in P1HA levels at POL, KAL, and TYF

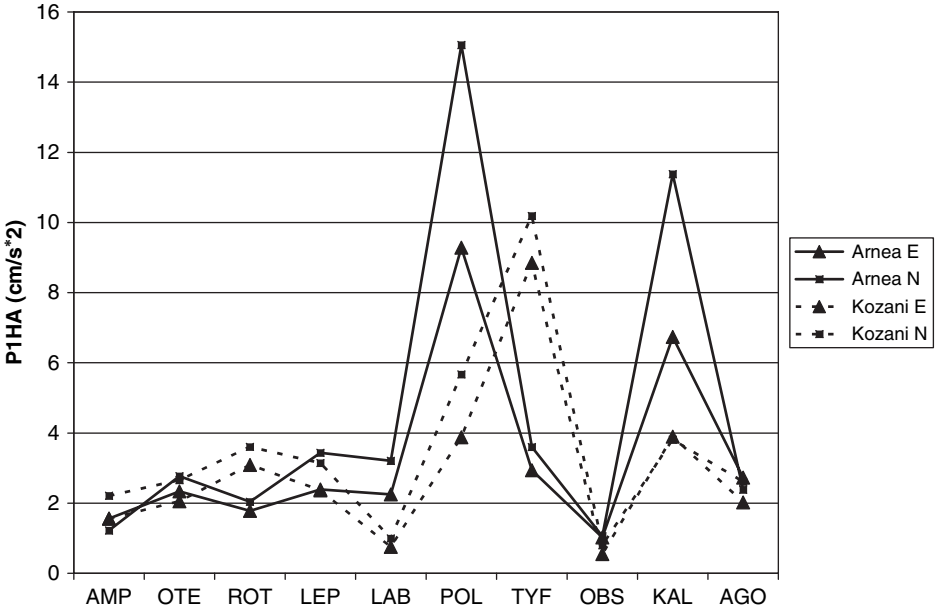

FIGURE 9 Graph with the largest estimated P1HA at the considered sites in the city of Thessaloniki due to the Arnea and Kozani 1995 earthquakes.

stations), a result that is also demonstrated by Triantafyllidis *et al*. [2002] and the engineers should be aware of this, in particular when designing high-risk buildings.

The uncertainty level of these results is estimated by varying in a narrow range the source parameters of the Arnea and Kozani events and computing the resulting P1HA variation in Thessaloniki. We compute for this purpose the P1HA values at the bedrock OBS site. We test 8 different models for the Arnea earthquake and 12 for the Kozani earthquake by slightly changing focal mechanisms, rupture propagation (choosing the nucleation of the two farthest limits of the faults), and seismic moment distribution (uniform and smoothed or with an asperity).

The results (Fig. 10) show strong variations (more than one order of magnitude) in the P1HA estimations only when the nucleation point changes and the rupture propagates towards the city of Thessaloniki (models 1÷4 for Arnea, models 7÷12 for Kozani). Although this directivity effect has a crucial role in source modeling and scenario estimations, its influence on the recording signals allows one to take this parameter in consideration beforehand. The variation in the P1HA related to other source parameters is within a factor of 4.

In Figure 11 the comparison between the bedrock signals and those obtained taking into account site effects at the station called "TYF" are shown. Since only the amplification in amplitude has been considered, the synthetic signals with and without site effects have the same shape and differ only in a frequency-dependent factor of amplification.

7. Conclusions

Peak accelerations at the maximum frequency of 1 Hz (P1HA) are estimated at ten selected localities within the city of Thessaloniki on the basis of source models derived for the 1995 earthquakes at Kozani and Arnea. The sources of the two events are modeled both as a point source and as a finite source. Since the related observed accelerograms did not have absolute timing nor a pre-trigger time, the modeling is done using a direct, trial and error approach.

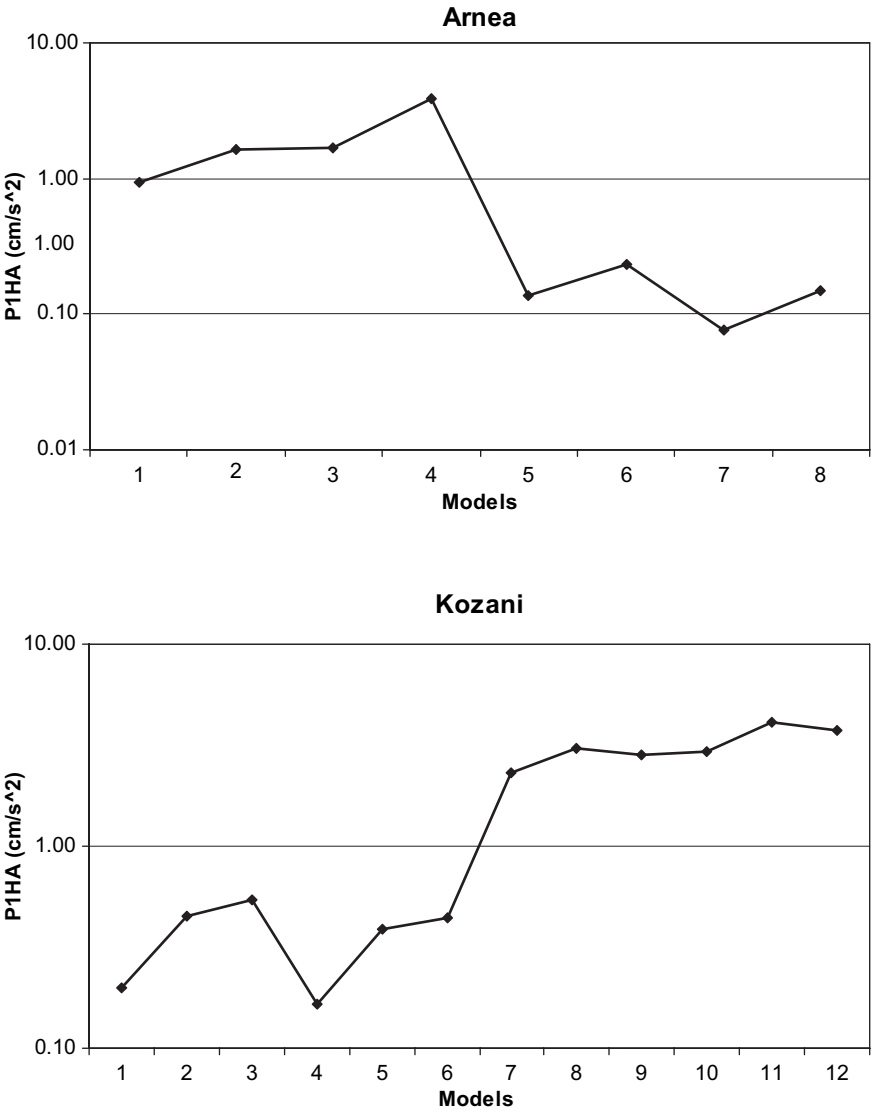

FIGURE 10 P1HA variation as a function of different models (see text) for Arnea (above) and Kozani events (below).

For the Arnea source modeling the highest analyzed frequency is 3 Hz. There were very few previous studies about this earthquake and due to the scarcity of recorded aftershocks not much information about the fault area was obtained. Moreover, only four registrations are available: two signals recorded at bedrock stations, two other with evident site amplification effects. Our analysis, based on both quantitative and qualitative criteria of comparing observed and synthetic data, led to the best solution obtained from a range of proposed models (best agreement in terms of peak 3 Hz accelerations). The point-source modeling provides the earthquake focal mechanism, $\theta = 260°$, $\delta = 42°$, $\lambda = -132°$, the hypocenter/centroid depth, 7 km, and the magnitude value, 5.8. The finite-source modeling provided the mainly E towards W almost unilateral rupture propagation, the fault area dimensions, either 10 km $\times$ 5 km or 13 km $\times$ 7 km, with the seismic moment distribution

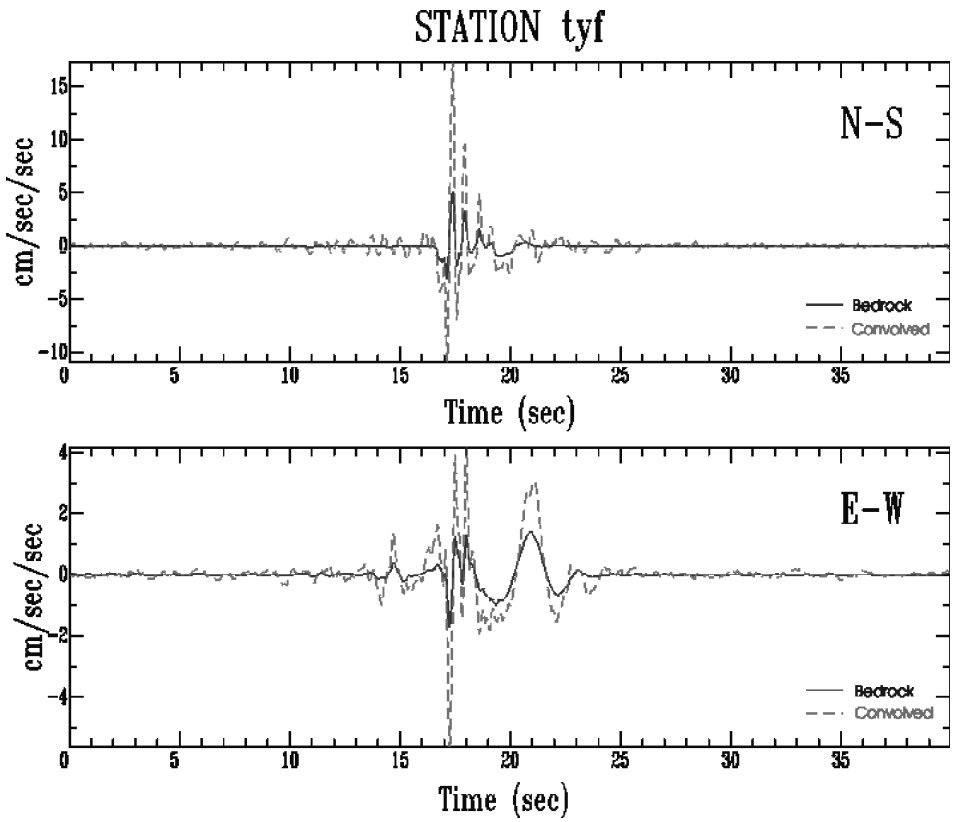

FIGURE 11 The synthetics seismograms due to the Arnea earthquake (computed using finite-source and applying 1-D structural model) at the station TYF in Thessaloniki with and without site effects.

being uniform and smoothed at the borders or characterized by one asperity modeled with the k^2 law, respectively. All these results are in agreement with previous studies [Margaris and Hatdizimitriou, 1997; Hatdizimitriou, 2003].

For the Kozani source modeling the upper frequency cutoff is 1 Hz. Eight strong motion stations recorded the earthquake, four of them not sited on bedrock. Previous studies and aftershocks locations suggested several parameters values for the source modeling. Our point-source modeling provides the focal mechanism, $\theta = 253°$, $\delta = 43°$, $\lambda = 265°$, the nucleation depth, 12 km, and the magnitude, 6.6. The one-fault finite-source modeling provides the NE towards SW rupture propagation, the fault area dimensions, 18 km $\times$ 9 km with the seismic moment distribution characterized by two asperities, the larger one located at NE, near Kozani. The two-fault finite-source modeling, characterized by the presence of an antithetic fault as proposed by Hatzfeld *et al*. [1997], leads to the main fault dimensions of 25 km $\times$ 17 km, and to the antithetic fault dimensions of 8 km $\times$ 5 km. The presence of the antithetic fault caused the synthetic signals to have a stronger contribution of high frequencies, in agreement with the observations. All our results are in agreement with previous studies [Clarke *et al*., 1997; Hatzfeld *et al*., 1997].

Using the derived source models we estimate the P1HA at ten sites within the city of Thessaloniki, where the earthquakes have not been recorded. Since average site effects, in terms of the amplitude amplification with frequency, have already been proposed for these sites by Triantafyllidis *et al*. [2001, 2002, 2004a,b], we convolve them with synthetic

accelerations computed on bedrock for the source models related to the Arnea and Kozani 1995 events.

The Arnea earthquake produces strong 1 Hz accelerations at POL and KAL sites, whereas the Kozani earthquake produces the strongest 1 Hz accelerations at TYF. The P1HA values due to the two earthquakes are similar at all other sites. Uncertainties in the P1HA estimates are derived by slightly varying the best source parameters. The directivity effect produces strong variations (one order of magnitude) and should be taken into consideration also in engineering practice. The change in other source parameters produces P1HA variations within a factor of 4.

This simple approach can be used to get rapid estimates of PA based on fast available source parameters and previously available estimates of site effects at known localities. It can also be used to forecast acceleration levels in forward modeling of earthquake scenarios. A validation of such fast estimates can be subsequently made by more detailed 2-D and 3-D combined modeling of source, propagation and site effects.

Acknowledgments

This work was performed in the framework of the EU contract EVG1-CT2001-00040: EUROSEISRISK — Seismic Hazard Assessment, Site Effects, and Soil Structure Interaction in an Instrumented Basin. We thank C. B. Papazachos for the velocity data provided and for fruitful discussions. Thanks are due to an anonymous reviewer whose comments helped us to considerably improve the article.

References

Abrahamson, N. A. and Silva, W. J. [1997]. "Empirical response spectral attenuation relations for shallow crustal earthquakes," *Seismological Research Letters*. **68**, 94–127.

Ambraseys, N. N., Simpson, K. A., and Bommer, J. J. [1996] "Prediction of horizontal response spectra in Europe," *Earthquake Engineering and Structural Dynamics*. **25**, 371–400.

Ambraseys, N. N. and Simpson, K. A. [1996] "Prediction of vertical response spectra in Europe," *Earthquake Engineering Structural Dynamics*. **25**, 401–412.

Ambraseys, N., Smit, P., Sigbjornsson, R., Suhadolc, P., and Margaris, B. [2002] "Internet-Site for European Strong-Motion Data," European Commission, Research-Directorate General, Environment and Climate Programme.

Ambraseys, N. N. and Douglas, J. [2003]. "Near-field horizontal and vertical earthquake ground motions," *Soil Dynamics and Earthquake Engineering* **23**, 1–18.

Ambraseys, N. N., Douglas, J., Sarma, S. K., and Smit, P. M. [2005]. "Equations for the estimations of strong ground motions from shallow crustal earthquakes using data from Europe and the Middle East: horizontal peak ground acceleration and spectral acceleration," *Bulletin Earthquake Engineering* **3**, 1–53.

Barka, A. and Reilinger, R. [1997] "Active tectonics of the Eastern Mediterranean region: deduced from GPS, neotectonic and seismicity data," *Annali di geofisica XL* **3**, 587–610.

Boatwright, J., Bundock, H., Luetgert, J., Seekins, L., Gee, L., and Lombard, P. [2003]. "The dependence of PGA and PGV on distance and magnitude inferred from Nothern California shakemap data," *Bulletin of the Seismological Society of America*. **93**, 2043–2055.

Bolt, B. A. [1987]. "*Seismic Strong Motion Synthetics*," Academic Press, Orlando, Florida, 328 pp.

Bolt, B. A. and Abrahamson, N. A. [2003]. "Estimation of strong seismic ground motion," In *International Handbook of Earthquake & Engineering Seismology*, Ed. Lee, H. K., Kanamori, H., Jennings P. C., and Kisslinger C. Eds. Academic Press, New York.

Boore, D. M., Joiner, W. B., and Fumal, T. E. [1997]. "Equation for estimating horizontal response spectra and peak acceleration from Western North American earthquakes: a summary of recent work," *Seismological Research Letters*. **68**, 128–153.

Campbell, K. W. [1981]. "Near-source attenuation of peak horizontal acceleration," *Bulletin of the Seismological Society of America*. **71**, 2039–2070.

Campbell, K. W. [1997]. "Empirical near source attenuation relationship for horizontal and vertical components of peak ground acceleration, peak ground velocity, and pseudo-absolute response spectra," *Seismological Research Letters*. **68**, 154–179.

Christodoulou, A. and Hatzfeld, D. [1988] "Three-dimensional crustal and upper mantle beneath Chalkidiki (Northern Greece)," *Earth and Planetary Science Letters*. **88**, 153–168.

Clarke, P. J., Paradissis, D., Briole, P., England, P. C., Parsons, B. E., Billiris, H., Veis, G., and Ruegg, J-C. [1997] "Geodetic investigation of 13 May 1995 Kozani-Grevena (Greece) earthquake," *Geophysical Research Letters.* **24**, 707–710.

Das, S., Suhadolc, P., and Kostrov, B. V. [1996] "Realistic inversions to obtain gross properties of the earthquake faulting process," In *Seismic Source Parameters: from Microearthquakes to Large Events*, Trifu, C. I. Ed. *Tectonophysics* **261**, 165–177.

Douglas, J. [2003]. "Earthquake ground motion estimation using strong-motion records: a review of equations for the estimation of peak ground acceleration and response spectral ordinates," *Earth-Sciences Reviews.* **61**, 43–104.

Douglas, J., Suhadolc, P., and Costa, G. [2004] "On the incorporation of the effect of crustal structure into empirical strong ground motion estimation," *Bulletin of Earthquake Engineering.* **2**, 75–99.

Drakatos, G., Papanastassiou, D., Voulgaris, N., and Stavrakakis, G. [1998] "Observations on the 3-D crustal velocity structure in the Kozani-Grevena (NW Greece) area," *Journal of Geodynamics.* **26**, 341–351.

Florsh, N., Fäh, D., Suhadolc, P., and Panza, G. F. [1991] "Complete Synthetic Seismograms for High Frequency Multimode SH-waves," *Pageoph.* **136**, 529–559.

Gusev, A. [1983]. "Descriptive statistical model of earthquake source radiation and its application to an estimate short-period strong motion," *Geophysical Journal of the Royal Astronomy Society*. **74**, 787–808.

Hadtzidimitriou, M. [2003] Personal communication.

Hatzfeld, D., Nord, J., Paul, A., Guiguet, R., Briole, P., Ruegg, J.-C., Cattin, R., Meyer, B., Hubert, A., Bernard, P., Makropulos, K., Karakostas, V., Papaioannou, C., Papanastassiou, D., and Veis, G. [1995] "The Kozani-Grevena (Greece) earthquake of May 13, 1995, M_S = 6.6. Preliminary results of a field multidisciplinary survey," *Seismological Research Letters*. **66**, 61–70.

Hatzfeld, D., Karakostas, V., Ziazia, M., Selvaggi, G., Lebogne, S., Berge, C., Guiguet, R., Paul, A., Voidomatos, P., Diagourtas, D., Kassaras, I., Koutsikos, I., Makropoulos, K., Azzara, R., Di Bona, M., Baccheschi, S., Bernard, P., and Papaioannou, C. [1997] "The Kozani-Grevena (Greece) earthquake of 13 May 1995 revisited from a detailed seismological study," *Bulletin of the Seismological Society of America*. **87** (2), 463–473.

Herrero, A. and Bernard, P. [1994] "Kinematics self-similar rupture process for earthquakes," *Bulletin of the Seismological Society of America*. **84** (4), 1216–1228.

Irikura, K. [1983]. "Semi-empirical estimation of strong ground motions during large earthquakes," *Bulletin of the Disaster Prevention Research Institute (Kyoto Univ.)* **33**, 63–104.

Irikura, K., Miyake, K., Iwata, T., Kamae, K., Kawabe, H., and Dalguer, L.A. [2004]. "Recipe for predicting strong ground motions from future large earthquakes," *13th World Conference of Earthquake Engineering*, Vancouver, Canada, Paper No. 1371.

Jansky, J. [1994] "HAD – Head And Direct waves. Program for computation of travel times and rays in layered media." Research report (in Czech), Dept. of Geophysics, Fac. of Mathemat. And Physics, Charles University, Prague.

Joyner, W. B. and Boore, D. M. [1981]. "Peak horizontal acceleration and velocity from strong ground motion records including records from the 1979 Imperial Valley, California, earthquake," *Bulletin of the Seismological Society of America*. **71**, 2011–2038.

Joyner, W. B. and Boore, D. M. [1988]. "Measurement, characteristics and prediction of strong ground motion," *Proceedings of the Specialty Conference on Earthquake Engineering and Soil Dynamics II*, ASCE Park City, Utah, 43–102.

Joyner, W. B. and Boore, D. M. [1993]. "Methods for regression analysis of strong motion data," *Bulletin of the Seismological Society of America*. **83**, 469–487.

Kanamori, H. and Anderson, L. [1975] "Theoretical basis of some empirical relations in seismology," *Bulletin of the Seismological Society of America*. **65** (5), 1073–1095.

Kanno, T., Narita, A., Morikawa, N., Fujiwara, H., and Fukushima, Y. [2006]. "A new attenuation relation for strong ground motion in Japan based on recorded data," *Bulletin of the Seismological Society of America*. **96**, 879–897.

Karagianni, E. E., Panagiotopoulos, D. G., Panza, G. F., Suhadolc, P., Papazachos, C. B., Papazachos, B. C., Kiratzi, A., Hatzfeld, D., Makropoulos, K., Priestley, K., and Vuan, A. [2002] "Rayleigh wave group velocity tomography in the Aegean area," *Tectonophysics* **358**, 187–209.

Margaris, B. N. and Hadtzidimitriou, M. [1997] "Source Parameters of the Arnea Earthquake, M_s = 5.8, Based on Stochastic Simulation Method," 3rd Hellenic conference on Geotechnical Engeneering, volume 1.

Marrara, F. and Suhadolc, P. [1998] "Observation and modeling of site effects in the Volvi basin (Greece)," in *The Effects of Surface Geology on Seismic Motion*, Irikura, K., Kudo, K., Okada, H., and Satasani, T. Eds., Balkema, Rotterdam, vol. 2, 973–980.

Meyer, B., Armjio, R., Massonet, D., De Chabalier, J.-B., Delacourt, C., Ruegg, J.-C., Achache, C., Briole, P., and Papanastassiou, D. [1996] "The Grevena (northern Greece) earthquake: fault model constrained with tectonic observation and SAR interferometry," *Geophysical Research Letters*. **23**, 2677–2680.

Mikumo, T. and Miyatake, T. [1987]. "Numerical modeling of realistic fault rupture process," in *Seismic Strong Motion Synthetics*, Bolt, B. A., Ed., Academic Press, New York.

Newmark, N. M. and Hall, W. J. [1982]. "Earthquake spectra and design," *Geotecnique* **25**, 139–160.

Novotny, O., Zahradnik, J., and Tselentis, G. A. [2001] "Northwestern Turkey Earthquakes and the Crustal Waves Observed in Western Greece," *Bulletin of the Seismological Society of America*. **91**, 875–879.

Panza, G. F. [1985] "Synthetic seismograms: the Rayleigh Waves Modal Sommation," *Journal of Geophysics* **58**, 125–145.

Panza, G. F. and Suhadolc, P. [1987] "Complete Strong Motion Synthetics," in *Seismic Strong Motion Synthetics*, Bolt, B. A., Ed., Academic Press, New York.

Papazachos, B. C., Comninakis, P. E., and Drakopoulos, J. C. [1966] "Preliminary results of an investigation of crustal structure in Southeastern Europe," *Bulletin of the Seismological Society of America*. **56**, 1241–1268.

Papazachos, C. B. [1998] "Crustal P and S velocity structure of the Serbomacedonian Massif (Nothern Greece) obtained by non linear inversion of traveltimes," *Geophysical Journal International*. **134**, 25–39.

Papazachos, C. B., Hatzidimitriou, P. M., Panagiotopoulos, D. G., and Tsokas, G. N. [1995] "Tomography of the crust and upper mantle in southeast Europe," *Journal of Geophysics Research*. **100**, 12405–12422.

Papazachos, C. B. and Nolet, G. [1997] "P and S deep velocity structure of the Hellenic area obtained by robust nonlinear inversion of travel times," *Journal of Geophysics Research*. **102**, 8349–8367.

Pavlides, S., Zauros, N. C., Chatzipetros, A. A., Kostopoulos, D. S., and Mountrakis, D. M. [1995] "The 13 May 1995 western Macedonia, Greece (Kozani Grevena) earthquake; preliminary results," *Terra Nova* **7**, 544–549.

Pitarka, A. [1999]. "3D elastic finite-difference modelling of seismic wave propagation using staggered grid with non-uniform spacing," *Bulletin of the Seismological Society of America*. **89**, 54–68.

Spudich, P., Joyner, W. B., Lindh, A. G., Boore, D. M., Margaris, B. M., and Fletcher, J. B. [1999]. "SEA99: a revised ground motion prediction relation for use in extensional tectonic regimes," *Seismological Society of America*. **89**, 1156–1170.

Triantafyllidis, P., Hatzidimitriou, P. M., and Suhadolc, P. [2001] "1-D theoretical modelling for site effects estimation in Thessaloniki – Comparison with observation," *Pageoph* **158**, 2333–2347.

Triantafyllidis, P., Suhadolc, P., and Hatzimitriou, D. [2002] "Influence of source on 2-D site effects," *Geophysical Research Letters*. **29** (6), 13, 1–4.

Triantafyllidis, P., Suhadolc, P., Hatzidimitriou, P. M., Anastasiadis, A. and Theodulidis, N. [2004a] "Theoretical site response estimation for microzoning purposes (Part I)," *Pageoph* **161**, 1185–1203.

Triantafyllidis, P., Suhadolc, P., Hatzidimitriou, P. M., Anastasiadis, A., and Theodulidis, N. [2004b] "Theoretical site response estimation for microzoning purposes (Part II)," *Pageoph* **161**, 1185–1203.

Tselentis, G. A. [1998] "Fault lenghts during the Patras 1993 earthquakes sequence as estimated from the pulse width of initial P wave," *Pure and Applied Geophysics*. **152**, 75–89.

Tselentis, G. A., Melis, N. S., Sokos, E., and Papasimpta, K. [1996] "The Egion June 15, 1995 (6.2 ML) earthquake, Western Greece," *Pure and Applied Geophysics*. **147**, 83–98.

Vidale, J. and Helmberger, D. V. [1987]. "Path effects in strong ground motion seismology," in *Seismic Strong Motion Synthetics*, Bolt, B. A., Ed., Academic Press, New York.

Youngs, R. R., Chiou, S. J., Silva, W. J., and Humphrey, J. R. [1997]. "Strong ground-motion relationship for subduction zones," *Seismological Research Letters.* **68**, 58–73.

Wells, D. and Coppersmith, K. [1994] "New empirical relationship among magnitude, rupture length, rupture width, rupture area, and surface displacement," *Bulletin of the Seismological Society of America*. **84** (4), 974–1002.

Zahradnik, J. and Papatsimpa, K. [2001] "Focal mechanism of weak earthquakes from amplitude spectra and polarities," *Pure and Applied Geophysics*. **158**, 647–665.

Zhao, J. X., Zhang, J., Asano, A., Ohno, Y., Oouchi, T., Takahashi, T., Ogawa, H., Irikura, K., Thio, H. K., Somerville, P.G., Fukushima, Ya, and Fukushima, Yo. [2006a]. "Attenuation relations of strong ground motion in Japan using site classification based on predominant period," *Bulletin of the Seismological Society of America*. **96**, 898–913.

Zhao, J. X., Irikura, K., Zhang, J., Fukushima, Ya., Somerville, P. G., Asano, A., Ohno, Y., Oouchi, T., Takahashi, T., and Ogawa, H. [2006b]. "An empirical site-classification method for strong-motion stations in Japan using H/V response spectral ratio," *Bulletin of the Seismological Society of America*. **96**, 914–925.